JOURNAL OF SPACECRAFT AND ROCKETS
Vol. 42, No. 2, March–April 2005

Stability of Flexible Spacecraft During a Shallow Aeroassist

Joseph R. Schultz* and Darryll J. Pines†
University of Maryland, College Park, Maryland 20740

For a spacecraft to make scientific measurements in the upper atmosphere, it might be necessary for the spacecraft to "dip" into the upper atmosphere. This aeroassist maneuver presents stability challenges that are compounded if the spacecraft contains long flexible booms. Several stability aspects that are unique to this flexible class of spacecraft undertaking an aeroassist are examined. Using a detailed, linear model, simple analytic equations are developed to predict the stability of spacecraft with two or four flexible booms in symmetric configurations. In general, rearward-positioned and rearward-oriented booms help stabilize the spacecraft, but the spacecraft becomes less stable as boom flexibility increases, particularly for forward oriented booms. Also, depending on the spacecraft body and boom parameters, there are some configurations where the booms actually bend forward into the flow and not backwards as might be expected.

Nomenclature

$\hat{a}$	=	boom reference frame unit directions
$\hat{b}$	=	body reference frame unit directions
b^*	=	damping constant
C_D	=	drag coefficient
C_L	=	lift coefficient
C_M	=	moment coefficient
$\bar{c}$	=	molecular thermal speed
I	=	moment of inertia
k	=	nondimensional boom spring constant (normalized by $1/2\rho V_o^2 S^* L^*$)
k^*	=	spring constant
L	=	nondimensional length of each boom (normalized by L^*)
L^*	=	length of the spacecraft body
m	=	mass ratio (mass of each boom normalized by m_{tot})
m_{tot}	=	mass of the entire spacecraft
O	=	boom connection point
P	=	center of mass
q	=	generalized coordinates
R_o	=	spacecraft's orbit radius
r	=	nondimensional distance of $\boldsymbol{r}_B$ (normalized by L^*)
$\boldsymbol{r}$	=	displacement from the boom's center of mass to the body connection point
$\boldsymbol{r}_B$	=	displacement from the body center of mass to the boom connection point
S	=	surface area ratio (surface area of each boom normalized by S^*)
S^*	=	cross-sectional surface area of the spacecraft body
$\hat{s}$	=	spacecraft reference frame unit directions
u	=	generalized velocities
V_o	=	spacecraft's orbit velocity
$\hat{w}$	=	wind reference frame unit directions
x_{AC}	=	nondimensional location of aerodynamic center (normalized by L^*)
γ	=	flight-path angle
ε	=	momentum rebound fraction
θ	=	deflection angle
ξ	=	diffuse to specular fraction
ρ	=	atmospheric density
ϕ	=	boom angle

Subscripts

b, B	=	spacecraft body
diff	=	diffuse gas-surface interaction
n	=	boom number
o	=	neutral position
spec	=	specular gas-surface interaction
x, y, z	=	x, y, z direction
α	=	slope at neutral position

I. Introduction

MOST satellites and spacecraft fly in high enough orbits so that they will not experience significant aerodynamic drag in an orbital time period. However, there are some missions where a spacecraft might wish to enter the upper regions of the Earth's atmosphere for a short period of time. These missions can be operational or scientific in nature, such as to conduct an aeroassist for an orbital plane change or to take magnetosphere readings in the upper atmosphere. Much of the literature on aeroassist maneuvers focuses on spacecraft with space-shuttle-like configurations, where the spacecraft is treated as a point-mass model.[1,2] Because of the rigid-body nature of these spacecraft, internal flexibility modes are usually not of concern. Spacecraft with long, flexible booms, however, present an extra layer of dynamics. Even in free space, instabilities can arise that would not normally be predicted by a point-mass model. Although the literature quite extensively covers the dynamics and control of these flexible spacecraft in free space,[3,4] there is little analysis when those types of spacecraft undergo the aerodynamic effects of an aeroassist.

This paper bridges that gap by developing a detailed linear model of a flexible class of spacecraft undergoing an aeroassist. With this model, both static and dynamic stability characteristics will be analyzed. Additionally, analytic solutions will be developed from the model to give a spacecraft designer a better feel for how changes to the spacecraft parameters affect the spacecraft's stability.

In the next section, a two-dimensional model of the spacecraft is developed. This is followed by a discussion of the aerodynamic forces encountered by a spacecraft in the upper atmosphere. Finally, stability properties are addressed for spacecraft configurations with two, four, or more flexible booms.

Received 10 March 2003; revision received 21 November 2003; accepted for publication 13 April 2004.

*Graduate Student, Department of Aerospace Engineering; currently Guidance Navigation and Controls Engineer, Swales Aerospace, Beltsville, MD 20705; jschultz@swales.com. Student Member AIAA.

†Associate Professor, 3181 Martin Hall, Department of Aerospace Engineering; djpterp@eng.umd.edu. Associate Fellow AIAA.

II. Spacecraft Model

For analysis of the problem, a two-dimensional, linear spacecraft model will be developed. Such a model provides an estimate of the dynamic behavior of the spacecraft. The benefits and limitations of the model will be discussed throughout the paper.

The spacecraft model consists of several rigid bodies with one being the main spacecraft body (body B) and the others being any number of booms (bodies A_n) attached to body B at various locations. Figure 1 shows a model of the spacecraft. For simplicity, only two booms are shown. (Note that $\hat{s}_x$ is the along-track orbit direction and $\hat{w}_x$ is the in-track orbit direction.)

To take advantage of classic stability and control analysis techniques, linearized equations of motion will be developed. The largest difficulty in this approach is to handle one of the major components of the aerodynamics, density, because it will vary exponentially with the orbit height of the spacecraft. Any linearization of the density as a variation of height will cause large errors when predicting the flight path of the satellite. However, if one limits the discussion to a study of the dynamics of the spacecraft itself and not on the stability of maintaining specific orbit paths, then a solution where density is held as a constant can be used. Later, when one knows that a particular spacecraft configuration meets the designer's particular stability needs, it is possible to move to a nonlinear or point-mass model such as one by London[1] or Vinh[2] to evaluate the flight-path requirements. It is likely that several of these iterations might be done during the entire design process.

To investigate the dynamic behavior of the spacecraft across the entire flight regime, snapshots at various altitudes (densities) can be taken. Of greatest interest is the altitude where the aerodynamics will have the greatest effect. This occurs at the spacecraft's perigee where it is at the bottom of its atmospheric dip. It is here where the dynamics are the most interesting, and it is here where all of the following analysis will take place. At the perigee point, the spacecraft's trajectory can be approximated as straight and level at a constant altitude. At this point of level flight, a flat-Earth dynamic model can be used without loss of detail. Assuming a flat-Earth model, the gravity force is omitted in the equations of motion. It will be assumed that any gravity-gradient forces affecting the spacecraft can be ignored in comparison to the aerodynamic force strength.

A. Structural Modeling of the Booms

The booms will be modeled as rigid bodies connected to the main body by a linear, torsional spring. This will capture the first mode of vibration in the dynamics. The angle between the boom and the body (ϕ_n in Fig. 1) can be comprised of the boom's undeflected or neutral position θ_{no} and the boom's deflection θ_n from this position:

$$\phi_n = \theta_{\text{no}} + \theta_n \tag{1}$$

To aid in linear analysis, it will be assumed that θ_n is small. The linear spring's reaction moment M_{Rn} between boom n and the main body is, classically,

$$\boldsymbol{M}_{\text{Rn}} = \left(-b_n^*\dot{\theta}_n - k_n^*\theta_n\right)\hat{s}_y \tag{2}$$

B. Aerodynamic Force Modeling

In many cases, the flight path of the spacecraft will be confined to an altitude of 120 km above the Earth's surface and higher in order to minimize drag and large heating rates. At these altitudes, a rarefied gas-surface interaction model will be needed. A rarefied aerodynamic model is appropriate for flows where the Knudson number is much greater than one (Ref. 5). Therefore, such a model is appropriate when a moderate-sized spacecraft is confined to fly 120 km above the Earth's surface and higher. If flight lower than 120 km is desired, a different aerodynamic model would be needed.

Lewis[6] and Bowman[7] provide formulas for lift and drag forces under diffuse and specular gas-surface interactions expected in rarefied flow. By converting their equations into the standard

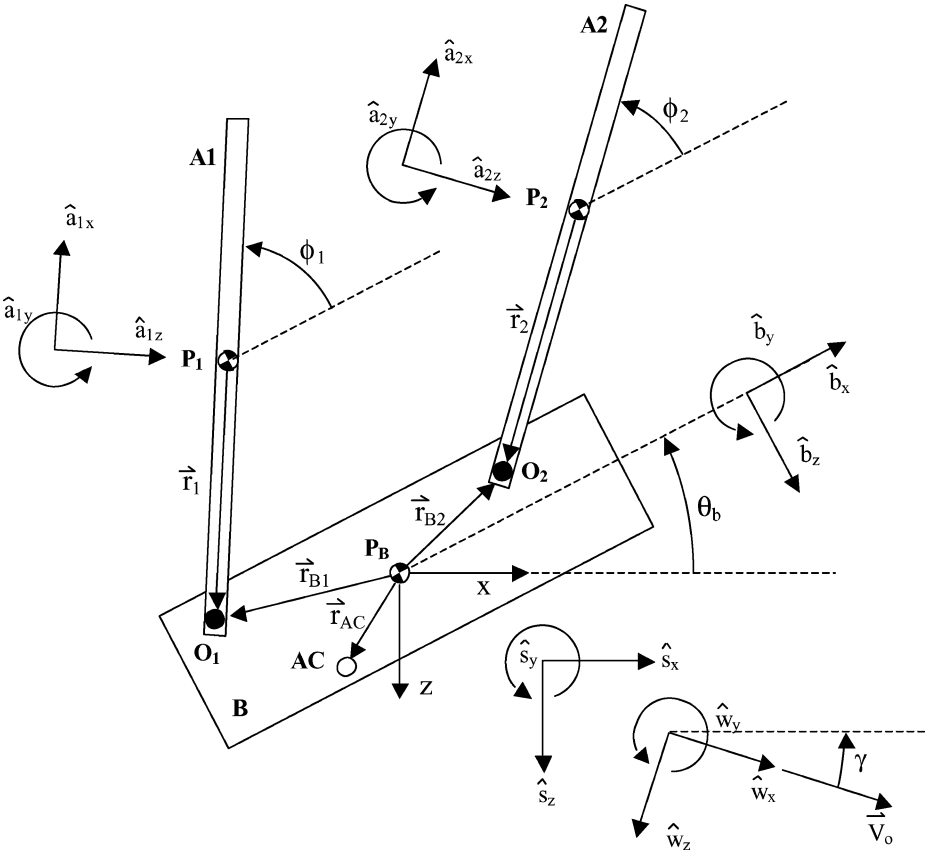

Fig. 1 Spacecraft model.

notation of

$$\text{Lift} = \tfrac{1}{2}\rho V_o^2 S^* C_L \tag{3a}$$

$$\text{Drag} = \tfrac{1}{2}\rho V_o^2 S^* C_D \tag{3b}$$

the lift and drag coefficients for a flat surface can be written as

$$C_{\text{Dspec}} = 2[\sin\alpha + \bar{c}/(4V_o)](1 - \varepsilon\cos 2\alpha) \tag{4a}$$

$$C_{\text{Lspec}} = 2[\sin\alpha + \bar{c}/(4V_o)]\varepsilon\sin 2\alpha \tag{4b}$$

$$C_{\text{Ddiff}} = 2[\sin\alpha + \bar{c}/(4V_o)]\left(1 + \varepsilon\tfrac{2}{3}\sin\alpha\right) \tag{4c}$$

$$C_{\text{Ldiff}} = 2[\sin\alpha + \bar{c}/(4V_o)]\varepsilon\tfrac{2}{3}\cos\alpha \tag{4d}$$

$$C_D = \xi C_{\text{Dspec}} + (1 - \xi)C_{\text{Ddiff}} \tag{5a}$$

$$C_L = \xi C_{\text{Lspec}} + (1 - \xi)C_{\text{Ldiff}} \tag{5b}$$

where α is the angle between a spacecraft surface and the incoming flow and $\bar{c}/V_o$ is the thermal speed ratio.

The spacecraft body, however, is typically a complex shape consisting of many flat surfaces. To find the overall lift and drag coefficients of the body using the preceding equations, the lift and drag could be calculated over each surface of the body and the results integrated to provide the overall lift and drag coefficients. However, such detail is beyond the scope of this paper, and it will be assumed that these values are already provided. Bowman[7] and Sentman[8] provide analysis that could be used to determine the coefficients of the body.

Fortunately, such detail is not necessary for the spacecraft booms. Under the gas-surface parameters that are likely to be encountered—high orbital speeds, small momentum rebound fraction, and diffuse behavior—surface features are effectively diminished, and the booms can be modeled as flat plates.[9] With the flat-plate assumption, Eqs. (4a–5b) will be used for the coefficients of the entire boom with α as the angle the booms make with the flow direction.

To comply with the linear form, the boom's lift and drag coefficients can be written as

$$C_L = C_{Lo} + C_{L\alpha}\alpha \tag{6a}$$

$$C_D = C_{Do} + C_{D\alpha}\alpha \tag{6b}$$

where the coefficients are calculated from Eqs. (4a–5b) at $\alpha = \theta_o$:

$$C_{Lo} = C_L|_{\alpha=\theta_o} \tag{7a}$$

$$C_{Do} = C_D|_{\alpha=\theta_o} \tag{7b}$$

$$C_{L\alpha} = \left.\frac{\partial C_L}{\partial\alpha}\right|_{\alpha=\theta_o} \tag{8a}$$

$$C_{D\alpha} = \left.\frac{\partial C_D}{\partial\alpha}\right|_{\alpha=\theta_o} \tag{8b}$$

C. Equations of Motion

The equations of motion can be generated using Kane's method,[10] which is the Lagrange form of d'Alembert's principle. For simplicity, a spacecraft with only two booms will be derived here. Once the equations of motion are generated for a two-boom spacecraft, the form of the equations will be readily apparent for a spacecraft of any number of booms. Later, results for a four-boom spacecraft will be shown but not derived.

The Appendix provides details for the development of the equations of motion for a two-boom spacecraft. The equations of motion that result can be placed in the state-space form of

$$\dot{\boldsymbol{x}} = A\boldsymbol{x} + \boldsymbol{x}_o \tag{9}$$

where the dependant variables in the $\boldsymbol{x}$ array are the nondimensionalized linear and angular accelerations and velocities of the spacecraft body and booms and the $\boldsymbol{x}_o$ array is a nondimensionalized force or torque per mass constant as described in the Appendix.

With this A matrix determined, one can examine its eigenvalues for dynamic stability analysis, investigate control issues, and conduct computer simulations. The elements of this A matrix are also summarized in the Appendix.

III. Stability Analysis

To examine the behavior of a flexible spacecraft undertaking an aeroassist, a spacecraft with just two booms in a symmetric configuration will be used for simplicity (Fig. 2). With this configuration, the booms are assumed to have identical properties. The spacecraft is assumed to be symmetric about the spacecraft body's centerline with its center of mass located on the centerline. The booms are also assumed to be placed together somewhere along the centerline. For the two-boom symmetric spacecraft configuration, it can be shown that Eq. (9) is in the form given in the Appendix [Eq. (A31)]. Many things can be ascertained from this simple model, which can be transferred to a spacecraft with more booms if desired. Figure 3 is an example of a symmetric four-boom spacecraft.

A. Quasi-Static Solution

In many applications, it is important to know how far booms will bend during the aeroassist. If the booms represent antenna or scientific instruments, proper alignment can be important, and knowledge of the boom position might be required for signal compensation.

To determine the amount of deflections the booms experience, a quasi-static solution can be found from the equations of motion for a two-boom spacecraft. This solution can be found by assuming the spacecraft is in stable and level flight so that there is no net pitching of the body or net vertical movement in the z direction. However, drag on the spacecraft will decelerate it, and that deceleration will still need to be captured: hence a quasi-static solution. By setting all of the states in Eq. (9) to zero except for the deceleration of the spacecraft and the boom deflections, the quasi-static solution can be found from Eq. (A31) to be

$$\begin{bmatrix} \ddot{x}/V_o \\ \theta_1 \\ \theta_2 \end{bmatrix} = \frac{1}{a_{49}^2 - a_{59}^2} \times \begin{bmatrix} \left(a_{49}^2 - a_{59}^2\right) & -a_{19}\left(a_{49} + a_{59}\right) & a_{19}\left(a_{49} + a_{59}\right) \\ 0 & -a_{49} & a_{59} \\ 0 & a_{59} & -a_{49} \end{bmatrix} \begin{bmatrix} x_{01} \\ x_{04} \\ -x_{04} \end{bmatrix} \tag{10}$$

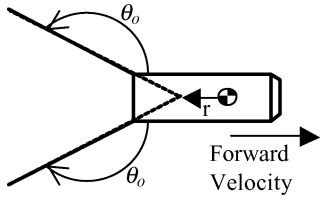

Fig. 2 Two-boom symmetric spacecraft.

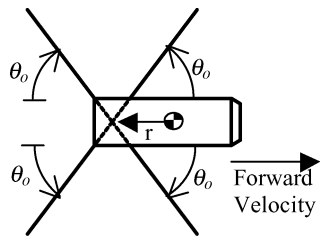

Fig. 3 Four-boom symmetric spacecraft.

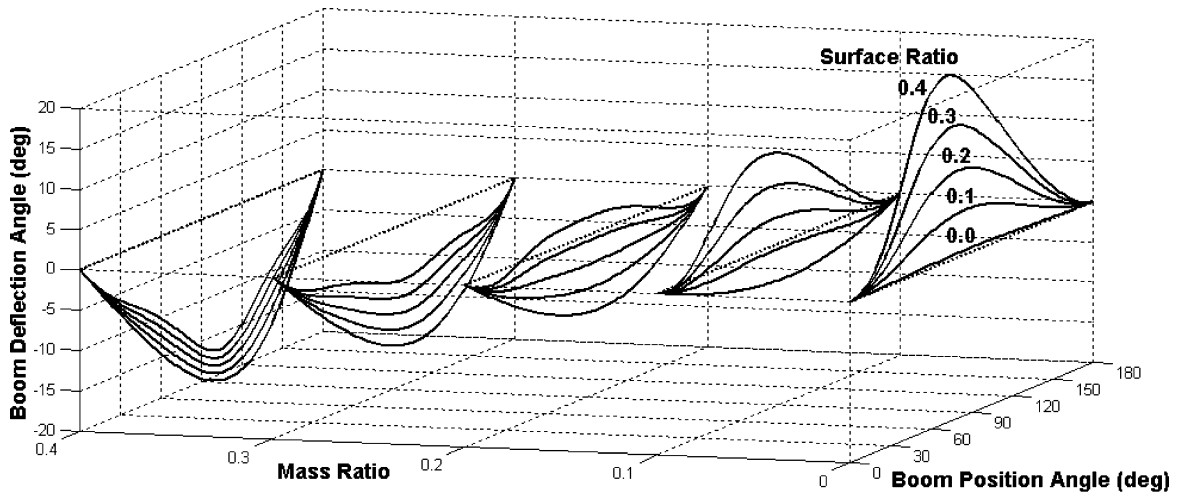

Fig. 4 Boom deflections for various ratios and position angles.

Or, simplifying for the deflections,

$$\theta_1 = -x_{04}/(a_{49} - a_{59}) \tag{11}$$

(Note that because of the symmetric nature, $\theta = \theta_1 = -\theta_2$.)

Substituting in the appropriate expressions and including the terms of the quasi-linear M matrix from the Appendix [Eq. (A27)], it can be shown that

$$\theta = -\frac{m_{11}b_{41} - (m_{14} + m_{24}q_4)b_{11}}{m_{11}k + m_{11}k_{43} - 2(m_{14} + m_{24}q_4)k_{14}} \tag{12}$$

Or, after substituting the appropriate variables,

$$\theta = \frac{[-(m/S)C_{\mathrm{Dbo}} + (1-2m)C_{Do}]s_{\theta o} + C_{Lo}c_{\theta o}}{2k/SL + [(m/S)C_{\mathrm{Dbo}} - (1-2m)C_{Do} - C_{L\alpha}]c_{\theta o} + [-1(1-2m)C_{D\alpha} + C_{Lo}]s_{\theta o}} \tag{13}$$

The coefficients C_{Lo}, C_{Do}, $C_{L\alpha}$, and $C_{D\alpha}$ are the aerodynamic coefficients that correspond to the top-most boom in the two-boom configuration. Also, $s_{\theta o}$ and $c_{\theta o}$ are abbreviations for $\sin(\theta_o)$ and $\cos(\theta_o)$, respectively.

The deflection of the booms depends only on a few variables and ratios: the mass ratio m, a ballistic coefficient-like ratio $(mC_{\mathrm{Dbo}})/S$, a spring constant ratio $(2k)/(SL)$, and the boom angle θ_o. For a given set of gas-surface interaction parameters, C_{Lo}, C_{Do}, $C_{L\alpha}$, and $C_{D\alpha}$ only depend on θ_o.

Figure 4 shows the boom deflections for several mass and surface ratios of the booms. For simplicity, C_{Dbo} was set to a value of 3, L at 2, and k at 4 for the graph.

It would be expected that as a result of the oncoming flow the booms would bend farther back (have a positive boom deflection angle). However, as one examines Fig. 4, there are many combinations of mass and surface ratios that lead to negative boom deflection angles: the booms bend forward into the flow. The reason for this is that one needs to take into account the fact that the body of the spacecraft is also experiencing deceleration caused by drag. For some combinations of ratios, the deceleration of the body is greater than that of the booms, and, thus relative to the body, the booms will end up deflecting forward. The absolute deceleration of the main body does not have to be large at all, but it just needs to be larger than the booms' for the booms to go forward. Whether or not the booms bend forward or back depends on the booms' and body's ballistic coefficients, $(mC_{\mathrm{Dbo}})/S$.

As seen by the graph, variations in the mass and surface-area ratios produce different boom deflections. The variation of the spring constant and body drag coefficient also result in changes to the curves but, generally, not the overall shape. Typically, the drag coefficient for the body could vary between two and four. In this range, the curves shown in the figure will not change very much in shape or amplitude, especially when m is small.

The variation of the spring constant, however, can bring out a dramatic change in the amplitude of the graphs. As expected, as the spring constant gets smaller, the booms will bend more. As the spring constant gets larger, the booms will bend less. In most cases, varying the spring constant does not change the shape of the curves, just the amplitudes. Still, one needs to be mindful of the linear approximations used in the analysis. If the spring constant is so small as to allow the booms to deflect a large amount, the equations might no longer be applicable.

B. Dynamic Stability

If a particular set of booms meets the static deflection requirements of the spacecraft, it is important to check that the booms will meet the spacecraft's dynamic stability requirements. Given a main body without extra stabilizing characteristics, it would be expected that a rearward-positioned, rearward-facing boom configuration would be stable and a forward-positioned, forward-facing boom configuration would be unstable. It is the same expectation that shooting an arrow with its tail feathers in the back produces nice, stable flight, but shooting it with the feathers in the front will cause erratic, unstable behavior. To see whether this is true, an eigenvalue analysis was conducted for various boom configurations. One can determine stability by calculating the eigenvalues of the A matrix in Eq. (9). If all of the eigenvalues are negative, then the system is stable. If there is one or more positive eigenvalues in the group, then the system is unstable. The goal is to derive an analytic solution that will predict the existence of positive eigenvalues and thus the stability of a spacecraft design.

Because there are no horizontal or vertical constraints on the spacecraft, there is no preferred horizontal or vertical position. Therefore, the A matrix will always have at least two eigenvalues of zero corresponding to the rigid-body modes of the spacecraft. There are also two eigenvalues corresponding to the velocity of the spacecraft. Because the maintenance of stable orbits is not being considered in this analysis, those translational eigenvalues will be ignored when determining the existence of the nonnegative eigenvalues that produce rotational and vibrational instabilities.

Finding the eigenvalues of a large matrix can be easily accomplished numerically with standard software packages. By generating the value of the determinant of the A matrix (where, in this equation,

I is the identity matrix),

$$\det(\lambda I - A) = 0 \tag{14}$$

a 10th-order polynomial is produced, and solving for λ provides the eigenvalues.

Determining the eigenvalues analytically, however, is both lengthy and difficult. The process can be greatly simplified if one considers only whether the eigenvalues are positive or negative, not on their exact values. Although features like settling time or peak amplitude will not be determined, at least the designer can see the dividing line between the stable and unstable spacecraft configurations. The polynomial also can be reduced to sixth order if the translational eigenvalues are removed.

By using Routh's stability criteria[11] on this sixth-order polynomial, the exact solution of the 10th-order polynomial can be avoided completely. Instead, several smaller inequalities are generated that need to be satisfied. Of the six inequalities that need to be satisfied, five are consistently satisfied with realistic spacecraft parameters (such as requiring mass to be positive, surface area positive, etc.). However, one of those inequalities is satisfied with only a certain set of spacecraft parameters. It is this inequality that determines the stability and provides an analytic solution to the stability problem. It can be shown that if the following inequality is satisfied by the following elements of the A matrix given in the Appendix,

$$[a_{38}a_{49} - (a_{48} + a_{58})a_{39}] > 0 \tag{15}$$

the spacecraft is stable.

Substituting in the appropriate expressions into the equation will produce a rather lengthy expression; however, it can be simplified if a couple of assumptions are made. The assumptions are that the mass of the booms is small, and the effective aerodynamic surface area of the booms is reasonably large, that is,

$$m \ll 1 \tag{16a}$$

$$S/(mC_{\mathrm{Db}o}) \gg 1 \tag{16b}$$

Under these assumptions, the result of Eq. (15) can be reduced and rearranged to

$$\frac{C_{\mathrm{Mb}\alpha}}{SL} < \frac{-\{[2k/SL - (2r/L)C_{Do}][(C_{D\alpha} - C_{Lo})s_{\theta o} + (C_{L\alpha} + C_{Do})c_{\theta o}] + (2r/L)(2k/SL)(C_{L\alpha} + C_{Do})\}}{[2k/SL - (C_{D\alpha} - C_{Lo})s_{\theta o} + (C_{L\alpha} + C_{Do})c_{\theta o}]} \quad \text{(two-boom case)} \tag{17}$$

Although not directly derived, a similar stability expression can be derived for the four-boom spacecraft configuration under the same assumptions:

$$\frac{C_{\mathrm{Mb}\alpha}}{SL} < \frac{-2\{[2k/SL - (2r/L)C_{Do}][(C_{D\alpha} - C_{Lo})s_{\theta o} + (C_{L\alpha} + C_{Do})c_{\theta o}]^2 + (2r/L)(2k/SL)^2(C_{L\alpha} + C_{Do})\}}{\{(2k/SL)^2 - [(C_{D\alpha} - C_{Lo})s_{\theta o} + (C_{L\alpha} + C_{Do})c_{\theta o}]^2\}} \quad \text{(four-boom case)} \tag{18}$$

All of the stability parameters in Eqs. (17) and (18) relate to the spacecraft booms except for one $C_{\mathrm{Mb}\alpha}$. This term comes from the aerodynamic moment produced on the body of the spacecraft as the body's angle to the incoming flow changes. That is, for the spacecraft body (written in linear form),

$$C_{\mathrm{Mb}} = C_{\mathrm{Mb}o} + C_{\mathrm{Mb}\alpha}(\theta_b + \gamma) \tag{19}$$

Note that for a symmetric spacecraft body $C_{\mathrm{Mb}o} = 0$.

Generally, for a symmetric spacecraft, when the moment slope coefficient $C_{\mathrm{Mb}\alpha}$ is negative, the spacecraft will produce a restoring moment to return the spacecraft to its neutral, level position (no angle of attack) if it is disturbed from that position, making it stable. If $C_{\mathrm{Mb}\alpha}$ is positive, the spacecraft will produce a moment, if disturbed, away from its neutral position, making it unstable. If the spacecraft had no booms, then this term alone would determine the spacecraft's stability. The booms, however, will affect the entire spacecraft's stability.

The term $C_{\mathrm{Mb}\alpha}$ is also an important spacecraft parameter because for a symmetric spacecraft body it can be shown[12] that the aerodynamic center, x_{AC} and $C_{\mathrm{Mb}\alpha}$ are related by the equation

$$C_{\mathrm{Mb}\alpha} = (C_{\mathrm{Db}o} + C_{\mathrm{Lb}\alpha})x_{\mathrm{AC}} \tag{20}$$

Thus, $C_{\mathrm{Mb}\alpha}$ is important in determining the aerodynamic center of the spacecraft if the location of the center of gravity is known.

IV. Dynamic Stability Results

Unless specified otherwise, the spacecraft and atmospheric parameters in Table 1 will be used to help discuss the stability results. These parameters are representative of a planned spacecraft design that will be discussed in the next section.

Using the analytic stability equations (17) and (18), the first study will look at which spacecraft body values of $C_{\mathrm{Mb}\alpha}$ are required for stability as boom location and orientation change. To simplify the study, the spring constant k will be set to a very large value (infinity) to simulate a rigid vehicle. This will show how the boom orientation and location normally play a role in overall spacecraft stability. Later, k will be shown for various values to show what role boom flexibility plays in stability.

A. Two-Boom Spacecraft

With k fixed at a large value for rigidity, Fig. 5 shows the stability for various values of $C_{\mathrm{Mb}\alpha}$, boom location, and boom orientation. Any value of $C_{\mathrm{Mb}\alpha}$ above a designated line in Fig. 5 produces an unstable configuration, whereas any value of $C_{\mathrm{Mb}\alpha}$ below a designated line produces a stable spacecraft configuration. Basically, with a given boom orientation and location, the spacecraft body will need to be designed to have its $C_{\mathrm{Mb}\alpha}$ lie below the appropriate line in order for the entire spacecraft to be stable.

As seen in the figure, a spacecraft with booms located near the front of the spacecraft (positive r values) tends to be less stable than one with booms located near the rear of the spacecraft (negative r values). Additionally, spacecraft with forward-angled booms (0–90 deg) generally tend to be less stable than those with rearward-angled booms (90–180 deg). This means that a spacecraft with

Table 1 Nominal spacecraft parameters

Variable	Value
L^*	5.0 m
L	2.0
S^*	1.0 m^2
S	0.2
k	4.0
r	−0.5
$C_{\mathrm{Db}o}$	3.0
$C_{\mathrm{Lb}\alpha}$	0.5
ε	0.2
ξ	0.1
$\bar{c}/V_o$	0.1

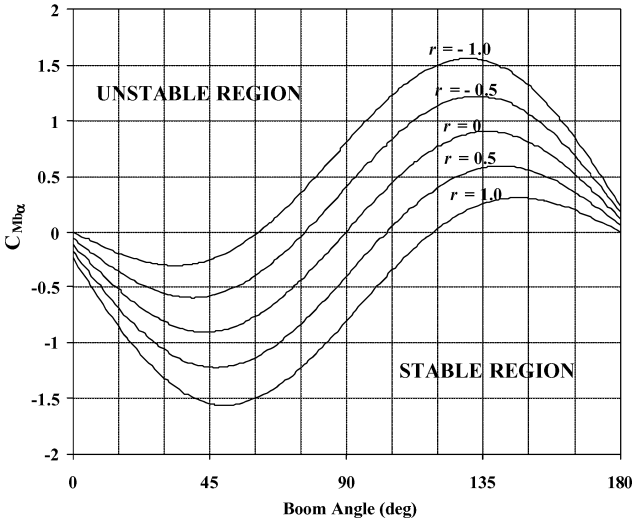

Fig. 5 Stability line for different boom locations, two booms, rigid.

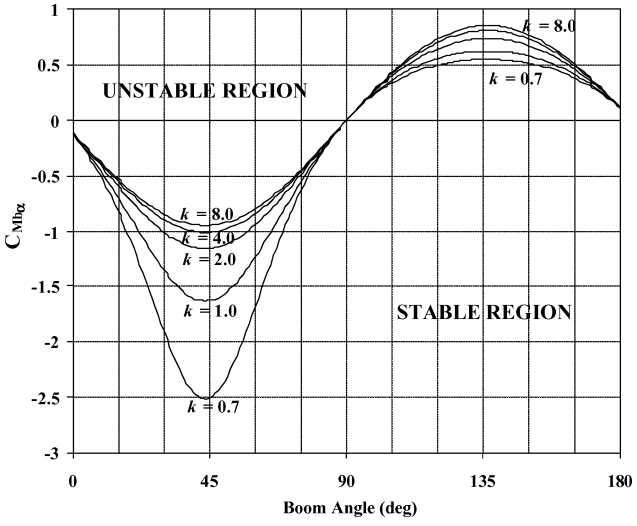

Fig. 6 Stability line for different spring constants, two booms, $r = 0$.

forward-facing booms near the front of the spacecraft will require a much more stable spacecraft body design (larger negative $C_{\mathrm{Mb}\alpha}$) than a spacecraft with booms near the rear and/or rearward-facing booms.

However, because this study concerns itself with flexible boom structures, it is important to look at how flexibility plays a role in stability. With the booms fixed to the body at the body's center of gravity ($r = 0$) for simplicity, Fig. 6 shows how the allowable range of $C_{\mathrm{Mb}\alpha}$ changes as k is varied to see what effect the boom stiffness plays in stability. (Note that similar graphs are produced for all ranges of r except that the results are translated up and down similar to Fig. 5.)

In general, the stiffer the booms, the more stable a spacecraft will be. Booms with a lower spring constant tend to destabilize the spacecraft. This effect is most pronounced when the booms are forward facing as compared to when they are rearward facing.

At a few boom angles, the $C_{\mathrm{Mb}\alpha}$ stability range line is the same for all values of boom spring constants. This occurs near 0, 90, and 180 deg. (These are the locations at all values of r, too.) This is because the aerodynamic forces that produce a moment at the spacecraft body through the spring do not change (linearly) when the boom angle changes slightly from these positions. Therefore, at these angles the contribution of the booms to the overall spacecraft stability is zero, and stability is independent of the boom stiffness. The stability requirements change the most near-boom angles of 45 and 135 deg because the aerodynamic moment from the booms has the greatest variance here as the boom angle changes. This moment change modifies the effective spring constant of the boom the most at these points, and hence the stability is affected the most.

It is also seen that the forward-facing booms are more sensitive to changes in k than rearward-facing booms. By examining the denominator of Eq. (17), one can see that the aerodynamic moment of the booms either adds or subtracts from spring constant. For forward-facing booms, the spring constant is effectively lowered; for rearward-facing booms, the spring constant is effectively increased. The aerodynamic moment is usually small compared to the spring moment, but if the spring moment is also small the resulting difference between the two orientations is pronounced. Hence it is easier to destabilize a spacecraft with forward-facing booms when the booms are very flexible.

Finally, it might be assumed that there is a correlation between boom deflection amounts and stability. Certainly, both depend on the value of k, but the correlation is not direct. The largest boom deflections occur near 90-deg boom orientations where a larger boom surface area is exposed; however, that is not where the largest stability differences occur with changing k. It is how the aerodynamic moments change the effective spring constant and not the boom deflections directly that determines stability.

B. Four-Boom Spacecraft

Similar analysis can be done for a spacecraft with four booms. With k fixed at a large value for rigidity, Fig. 7 shows the stability for various values of $C_{\mathrm{Mb}\alpha}$, boom locations, and boom orientations for a four-boom spacecraft. As with the two-boom spacecraft, a four-boom spacecraft with booms located near the front of the spacecraft tends to be less stable than one with booms located near the rear of the spacecraft.

With the four-boom spacecraft, however, there is no net forward-facing or rearward-facing orientation. There are always two booms facing forward and two booms facing rearward. Because of this, when $r = 0$ for a rigid spacecraft, there is no boom angle that is more or less stable than another in the four-boom configuration. If the booms are attached to the rear of the body's center of gravity ($r < 0$), then the spacecraft gets more stable as the booms get more perpendicular, but if $r > 0$, then the spacecraft gets less stable as the booms get more perpendicular. Therefore, boom positioning plays more of an interesting role in stability than in the two-boom case.

As with the two-boom case, the four-boom case can also be examined under flexible boom conditions. With r fixed at 0 for simplicity, Fig. 8 shows how the allowable range of $C_{\mathrm{Mb}\alpha}$ changes as k is varied to see what effect the boom stiffness plays in stability. Again, booms

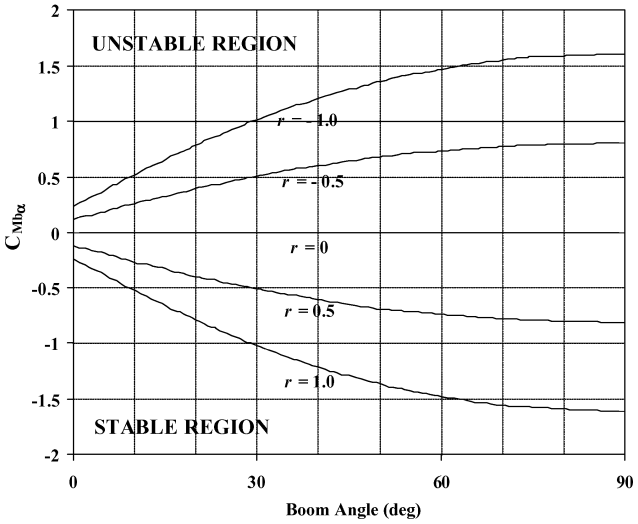

Fig. 7 Stability line for different boom locations, four booms, rigid.

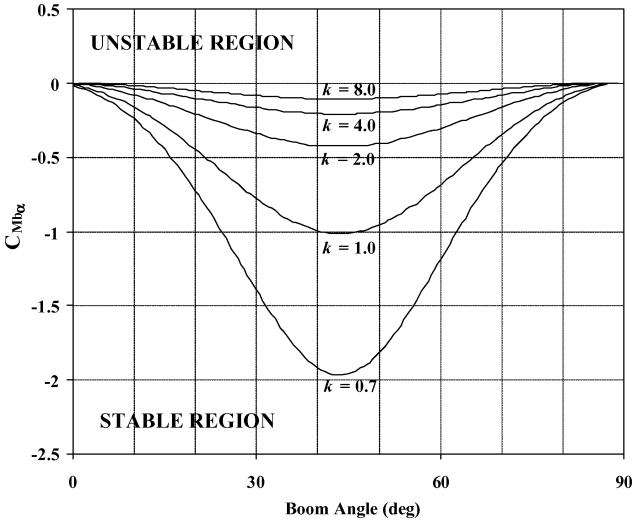

Fig. 8 Stability line for different spring constants, four booms, $r = 0$.

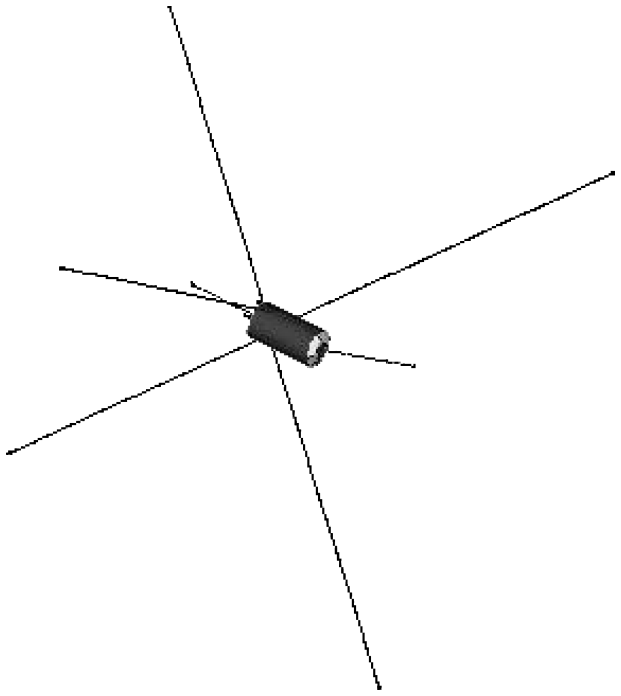

Fig. 9 GEC spacecraft (courtesy NASA Goddard).

with a lower spring constant tend to destabilize the spacecraft. The same discussion on the aerodynamic moment produced from the booms also applies. The effect on the spring constant is greatest when the booms are near 45 deg in the flow with minimal effect when they are at 0 or 90 deg.

C. Six-Boom Spacecraft in Orthogonal Configuration

The results from the two- and four-boom cases can used as a guide to investigate the stability of six-boom spacecraft proposed by NASA Goddard. The Geospace Electrodynamics Connections Mission (GEC)[13] spacecraft currently being designed by NASA at Goddard is a key example of a flexible spacecraft undergoing a shallow atmospheric pass. Its goal is to measure the Earth–sun electromagnetic interaction near the Earth.

The spacecraft has six long booms that hold instruments that measure the local electrical and magnetic field. An illustration of the spacecraft is shown in Fig. 9. One of the key missions of the spacecraft is to dip into the upper atmosphere (approximately 130 km above the Earth's surface) to take field readings at those altitudes. In this rarefied atmospheric region there will be significant aerodynamic loading on the booms and spacecraft. A potential concern is that the booms may cause instabilities.

The boom positions for the GEC configuration are fixed in an orthogonal arrangement with four booms at 45-deg angles in the pitching plane and two booms at 90-deg angles in the yawing plane. Because there are booms placed at 45-deg angles to the flow, boom stiffness will play a significant factor in determining the overall stability of the spacecraft as seen in both the two- and four-boom examples.

Three options could mitigate any stability problems: make $C_{Mb\alpha}$ more negative, increase k, or use a different boom configuration. The first could be accomplished by moving more of the weight of the spacecraft forward to increase x_{ac}, which would make $C_{Mb\alpha}$ a larger negative value. The second could be accomplished by increasing the stiffness of the four booms in pitch plane. And for the third option, the orthogonal configuration that is least sensitive to boom stiffness is where the four booms in the pitch plane have two booms at a 0-deg angle and two booms at a 90-deg angle to the flow.

The exact analytic relationship of the stability variables in the six-boom configuration is more complex to derive because of the aerodynamic coupling between the pitch and yaw planes, but it is expected that the same trends derived for the two- and four-boom configurations will be seen. Coupled stability equations for the six-boom orthogonal configuration will need to be developed in order to confirm these trends, and the development of those equations will be the goal of future research in the area.

V. Conclusions

This paper developed a viable first-order model to address the stability concerns of a flexible spacecraft undergoing an aeroassist maneuver. The resulting analytic solutions make it easier to predict and understand how changing a spacecraft parameter affects its stability. Although they are linear approximations, they provide more physical insight than what numerical solutions can provide. Both quasi-static solutions and dynamic stability characteristics can be studied for several flexible spacecraft configurations.

For spacecraft with attached booms, the boom deflections during an aeroassist can be predicted from the quasi-static stability equation. During flight through the atmosphere, the spacecraft's booms might not always bend backwards as one might expect. The deflections will depend on the spacecraft's properties. With large boom mass ratios and low boom surface-area ratios, the booms might actually bend forward in flight.

For most spacecraft, however, the main body of the spacecraft is much more massive than the booms, but the booms have a reasonable amount of surface area exposed to the airflow. Under these conditions, analytic solutions were found to predict the dynamic stability or instability of a particular spacecraft design.

In general, rearward-positioned and rearward-facing booms were more stable than booms located near the front of the spacecraft or those that were forward facing. Additionally, spacecraft configurations become less stable as the booms' spring constants become lower. This effect is most prominent when the booms are forward facing. In particular, the stability sensitivity is greatest when the booms are configured in a 45-deg angle with the flow.

Appendix: Derivation

Kane's method[10] is used to generate the equations of motion for a two-boom spacecraft. For a two-boom spacecraft in two dimensions, five generalized coordinates and five generalized velocities are needed to describe the system. Referring to Fig. 1, define

$$q_1 = (x - V_o t)/R_o \tag{A1a}$$

$$q_2 = (z - R_o)/R_o \tag{A1b}$$

$$q_3 = \theta_b \tag{A1c}$$

$$q_4 = \theta_1 \tag{A1d}$$

$$q_5 = \theta_2 \tag{A1e}$$

$$u_1 = (\dot{x} - V_o)/V_o \tag{A2a}$$

$$u_2 = \dot{z}/V_o \tag{A2b}$$

$$u_3 = \dot{\theta}_b \tag{A2c}$$

$$u_4 = \dot{\theta}_b + \dot{\theta}_1 \tag{A2d}$$

$$u_5 = \dot{\theta}_b + \dot{\theta}_2 \tag{A2e}$$

with t as time and θ_1 and θ_2 defined by Eq. (1). Such a selection will aid in linearizing the equations of motion because those generalized coordinates and velocities will typically take on small values.

The angular and linear velocity of each body member's center of gravity is

$${}^s\boldsymbol{\omega}_{\mathrm{PB}} = u_3\hat{s}_y \tag{A3a}$$

$${}^s\boldsymbol{\omega}_{\mathrm{Pn}} = u_{3+n}\hat{s}_y \tag{A3b}$$

$${}^s\boldsymbol{r}_{\mathrm{PB}} = (V_o u_1 + V_o)\hat{s}_x + (V_o u_2)\hat{s}_z \tag{A3c}$$

$${}^s\boldsymbol{r}_{\mathrm{Pn}} = (V_o u_1 + a_n u_3 + c_n u_{3+n} + V_o)\hat{s}_x + (V_o u_2 + b_n u_3 + d_n u_{3+n})\hat{s}_z \tag{A3d}$$

where, for $n = 1, 2$

$$a_n = r_{\mathrm{Bnz}} c_{q3} - r_{\mathrm{Bnx}} s_{q3} \tag{A4a}$$

$$c_n = -(L_n/2)\left[s_{\theta no + q(3+n)} c_{q3} + c_{\theta no + q(3+n)} s_{q3}\right] \tag{A4b}$$

$$b_n = -r_{\mathrm{Bnx}} c_{q3} - r_{\mathrm{Bnz}} s_{q3} \tag{A4c}$$

$$d_n = -(L_n/2)\left(c_{\theta no + q(3+n)} c_{q3} - s_{\theta no + q(3+n)} s_{q3}\right) \tag{A4d}$$

[Note that s_x and c_x are abbreviations for $\sin(x)$ and $\cos(x)$, respectively.]

The partial velocities are chosen to be

$$\begin{array}{cccccc} & u_1 & u_2 & u_3 & u_{3+n} & \\ \boldsymbol{v}^{\mathrm{PB}} & V_o\hat{s}_x & V_o\hat{s}_z & 0 & 0 & \\ \boldsymbol{v}^{\mathrm{Pn}} & V_o\hat{s}_x & V_o\hat{s}_z & a_n\hat{s}_x + b_n\hat{s}_z & c_n\hat{s}_x + d_n\hat{s}_z & \\ \boldsymbol{\omega}^{\mathrm{PB}} & 0 & 0 & \hat{s}_y & 0 & \\ \boldsymbol{\omega}^{\mathrm{Pn}} & 0 & 0 & 0 & \hat{s}_y & \end{array} \tag{A5}$$

The velocities and partial velocities can be linearized by replacing the a, b, c, and d terms in Eqs. (A4a–A4d) by their linear expressions:

$$a_n = r_{\mathrm{Bnz}} - r_{\mathrm{Bnx}} q_3 \tag{A6a}$$

$$c_n = -(L_n/2)(s_{\theta no} + c_{\theta no} q_3 + c_{\theta no} q_{3+n}) \tag{A6b}$$

$$b_n = -r_{\mathrm{Bnx}} - r_{\mathrm{Bnz}} q_3 \tag{A6c}$$

$$d_n = -(L_n/2)(c_{\theta no} - s_{\theta no} q_3 - s_{\theta no} q_{3+n}) \tag{A6d}$$

The full linearization of the terms will occur if the terms q_3, q_4, and q_5 are dropped in the preceding equations [(A6a–A6d)]. However, this quasi-linear form will be needed in the quasi-static deflection analysis. The simpler full linearization, though, is all that is needed for the dynamic stability analysis.

The accelerations in the generalized form are

$${}^s\dot{\boldsymbol{\omega}}_{\mathrm{PB}} = \dot{u}_3\hat{s}_y \tag{A7a}$$

$${}^s\dot{\boldsymbol{\omega}}_{\mathrm{Pn}} = \dot{u}_{3+n}\hat{s}_y \tag{A7b}$$

$${}^s\ddot{\boldsymbol{r}}_{\mathrm{PB}} = V_o\dot{u}_1\hat{s}_x + V_o\dot{u}_2\hat{s}_z \tag{A7c}$$

$${}^s\ddot{\boldsymbol{r}}_{\mathrm{Pn}} = (V_o\dot{u}_1 + a_n\dot{u}_3 + c_n\dot{u}_{3+n})\hat{s}_x + (V_o\dot{u}_2 + b_n\dot{u}_3 + d_n\dot{u}_{3+n})\hat{s}_z \tag{A7d}$$

The inertial forces can be written as

$$\boldsymbol{R}^*_{\mathrm{PB}} = -m_b\,{}^s\ddot{\boldsymbol{r}}_{\mathrm{PB}} \tag{A8a}$$

$$\boldsymbol{R}^*_{\mathrm{Pn}} = -m_n\,{}^s\ddot{\boldsymbol{r}}_{\mathrm{Pn}} \tag{A8b}$$

$$\boldsymbol{T}^*_{\mathrm{PB}} = -I_b\,{}^s\dot{\boldsymbol{\omega}}_{\mathrm{PB}} \tag{A8c}$$

$$\boldsymbol{T}^*_{\mathrm{Pn}} = -I_n\,{}^s\dot{\boldsymbol{\omega}}_{\mathrm{Pn}} \tag{A8d}$$

The generalized inertial forces are generated by (for $m = 1, \ldots, 5$)

$$F^*_m = \boldsymbol{v}^{\mathrm{PB}}_m \cdot \boldsymbol{R}^*_{\mathrm{PB}} + \boldsymbol{v}^{P1}_m \cdot \boldsymbol{R}^*_{P1} + \boldsymbol{v}^{P2}_m \cdot \boldsymbol{R}^*_{P2} + \boldsymbol{\omega}^{\mathrm{PB}}_m \cdot \boldsymbol{T}^*_{\mathrm{PB}} + \boldsymbol{\omega}^{P1}_m \cdot \boldsymbol{T}^*_{P1} + \boldsymbol{\omega}^{P2}_m \cdot \boldsymbol{T}^*_{P2} \tag{A9}$$

The spring-moment torques are

$$\boldsymbol{T}^S_{\mathrm{PB}} = [k_1 q_4 + k_2 q_5 + b_1(u_4 - u_3) + b_2(u_5 - u_3)]\hat{s}_2 \tag{A10a}$$

$$\boldsymbol{T}^S_{\mathrm{Pn}} = -[k_n q_{3+n} + b_n(u_{3+n} - u_3)]\hat{s}_2 \tag{A10b}$$

Similarly, the generalized spring moment forces F^S are generated by Eq. (A9) but replacing the * superscript with the S superscript.

The aerodynamic forces are (in the w frame)

$$\boldsymbol{R}^A_{\mathrm{PB}} = -\tfrac{1}{2}\rho V^2_{\mathrm{PB}} S_b C_{\mathrm{Db}}\hat{w}_x - \tfrac{1}{2}\rho V^2_{\mathrm{PB}} S_b C_{\mathrm{Lb}}\hat{w}_z \tag{A11a}$$

$$\boldsymbol{R}^A_{\mathrm{Pn}} = -\tfrac{1}{2}\rho V^2_{\mathrm{Pn}} S_n C_{\mathrm{Dn}}\hat{w}_x - \tfrac{1}{2}\rho V^2_{\mathrm{Pn}} S_n C_{\mathrm{Ln}}\hat{w}_z \tag{A11b}$$

With the rarefied gas aerodynamic model and assumed constant shape and size throughout the boom's length, there is no aerodynamic torque acting on the boom's center of mass. However, there might be an aerodynamic torque acting on the spacecraft body's center of mass. This can be expressed either by the lift and drag of the body acting about an aerodynamic center, or by a separate torque moment about the body's center of gravity as follows:

$$\boldsymbol{T}^A_{\mathrm{PB}} = (x_{\mathrm{ac}}\hat{b}_x + z_{\mathrm{ac}}\hat{b}_z) \times \left(-\tfrac{1}{2}\rho V^2_{\mathrm{PB}} S_b C_{\mathrm{Db}}\hat{w}_x - \tfrac{1}{2}\rho V^2_{\mathrm{PB}} S_b C_{\mathrm{Lb}}\hat{w}_z\right) = \tfrac{1}{2}\rho V^2_{\mathrm{PB}} S_b L_b C_{\mathrm{Mb}}\hat{w}_y \tag{A12}$$

The airflow velocities at each body's center of mass can be approximated by

$$V^2_{\mathrm{PB}} = V^2_o + 2V^2_o u_1 \tag{A13a}$$

$$V^2_{\mathrm{Pn}} = V^2_o + 2V^2_o u_1 + 2V_o a_n u_3 + 2V_o c_n u_{3+n} \tag{A13b}$$

where the a and c terms are as defined earlier.

The flight-path angle is approximated by

$$\gamma = \tan^{-1}\frac{V_z}{V_x} \approx \frac{V_z}{V_x} = \frac{V_o u_2}{V_o u_1 + V_o} = \frac{u_2}{u_1 + 1} \approx u_2 \tag{A14}$$

The lift and drag coefficients are linearized by

$$C_{\mathrm{Db}} = C_{\mathrm{Db}o} + C_{\mathrm{Db}\alpha}\alpha_b \tag{A15a}$$

$$C_{\mathrm{Lb}} = C_{\mathrm{Lb}o} + C_{\mathrm{Lb}\alpha}\alpha_b \tag{A15b}$$

$$C_{\mathrm{Dn}} = C_{\mathrm{Dn}o} + C_{\mathrm{Dn}\alpha}\alpha_n \tag{A15c}$$

$$C_{\mathrm{Ln}} = C_{\mathrm{Ln}o} + C_{\mathrm{Ln}\alpha}\alpha_n \tag{A15d}$$

where

$$\alpha_b = \gamma + \theta_b = u_2 + q_3 \tag{A16a}$$

$$\alpha_n = \gamma + \theta_b + \theta_n = u_2 + q_3 + q_{3+n} \tag{A16b}$$

With the substitutions and conversion to the s frame, the generalized aerodynamic forces can be similarly computed by Eq. (A9) but replacing the * superscript with the A superscript.

The equations of motion are generated by setting

$$\boldsymbol{F}^* + \boldsymbol{F}^A + \boldsymbol{F}^S = 0 \tag{A17}$$

The result is an expression in the form

$$\boldsymbol{M}\ddot{\boldsymbol{u}} = \boldsymbol{B}\boldsymbol{u} + \boldsymbol{K}\boldsymbol{q} + \boldsymbol{f}_o \tag{A18}$$

For a two-boom, symmetric spacecraft, many simplifications can be made. The symmetric spacecraft will have a boom configuration as pictured in Fig. 2. The booms are assumed to have identical properties. The spacecraft is assumed to be symmetric about the spacecraft body's centerline with its center of mass located on the centerline. The booms are also assumed to be placed at the same location somewhere along the centerline. For this type of spacecraft, the matrices will assume the following form:

$$M = m_{\text{tot}} L^{*2} \begin{bmatrix} m_{11} & 0 & 0 & m_{14} & -m_{14} \\ 0 & m_{11} & m_{23} & m_{24} & m_{24} \\ 0 & m_{23} & m_{33} & m_{34} & m_{34} \\ m_{14} & m_{24} & m_{34} & m_{44} & 0 \\ -m_{14} & m_{24} & m_{34} & 0 & m_{44} \end{bmatrix} \tag{A19}$$

$$K = -\frac{1}{2}\rho V_o^2 S^* L^* \begin{bmatrix} 0 & 0 & k_{13} & k_{14} & -k_{14} \\ 0 & 0 & k_{23} & k_{24} & k_{24} \\ 0 & 0 & k_{33} & k_{34} - k & k_{34} - k \\ 0 & 0 & k_{43} & k_{43} + k & 0 \\ 0 & 0 & k_{43} & 0 & k_{43} + k \end{bmatrix} \tag{A20}$$

$$B = -\frac{1}{2}\rho V_o^2 S^* L^* \begin{bmatrix} b_{11} & k_{13} & 0 & b_{14} & -b_{14} \\ 0 & b_{22} & 0 & b_{24} & b_{24} \\ 0 & k_{33} & 2b & b_{34} - b & b_{34} - b \\ b_{41} & k_{43} & -b & b_{44} + b & 0 \\ -b_{41} & k_{43} & -b & 0 & b_{44} + b \end{bmatrix} \tag{A21}$$

$$\boldsymbol{f}_o = -\frac{1}{2}\rho V_o^2 S^* L^* \frac{1}{2} \begin{bmatrix} f_{11} \\ 0 \\ 0 \\ f_{41} \\ -f_{41} \end{bmatrix} \tag{A22}$$

The matrix coefficients are

$$m_{11} = \frac{V_o^2}{L^{*2}} \tag{A23a}$$

$$m_{14} = -\left(\frac{V_o}{L^*}\right) m \left(\frac{L}{2}\right) s_{\theta o} \tag{A23b}$$

$$m_{23} = -2\left(\frac{V_o}{L^*}\right) mr \tag{A23c}$$

$$m_{24} = -\left(\frac{V_o}{L^*}\right) m \left(\frac{L}{2}\right) c_{\theta o} \tag{A23d}$$

$$m_{33} = I_b^* + 2mr^2 \tag{A23e}$$

$$m_{34} = m\left(\frac{L}{2}\right) r c_{\theta o} \tag{A23f}$$

$$m_{35} = -m\left(\frac{L}{2}\right) r s_{\theta o} \tag{A23g}$$

$$m_{44} = \tfrac{1}{3} m L^2 \tag{A23h}$$

$$b_{11} = 2\left(\frac{V_o}{L^*}\right)(C_{\text{Db}o} + 2SC_{Do}) \tag{A24a}$$

$$b_{14} = -SLC_{Do} s_{\theta o} \tag{A24b}$$

$$b_{24} = -SLC_{Lo} s_{\theta o} \tag{A24c}$$

$$b_{22} = \left(\frac{V_o}{L^*}\right)[(C_{\text{Db}o} + C_{\text{Lb}\alpha}) + 2S(C_{Do} + C_{L\alpha})] \tag{A24d}$$

$$b_{41} = -SL(C_{Do} s_{\theta o} + C_{Lo} c_{\theta o}) \tag{A24e}$$

$$b_{34} = \left(\frac{L^*}{V_o}\right) SLr C_{Lo} s_{\theta o} \tag{A24f}$$

$$b_{44} = \left(\frac{L^*}{V_o}\right) S\left(\frac{L^2}{2}\right)(C_{Do} s_{\theta o} + C_{Lo} c_{\theta o}) s_{\theta o} \tag{A24g}$$

$$k_{13} = \left(\frac{V_o}{L^*}\right) C_{\text{Db}\alpha} \tag{A25a}$$

$$k_{14} = \left(\frac{V_o}{L^*}\right) SC_{D\alpha} \tag{A25b}$$

$$k_{23} = \left(\frac{V_o}{L^*}\right)(C_{\text{Lb}\alpha} + 2SC_{L\alpha}) \tag{A25c}$$

$$k_{24} = \left(\frac{V_o}{L^*}\right) SC_{L\alpha} \tag{A25d}$$

$$k_{34} = -SrC_{L\alpha} \tag{A25e}$$

$$k_{33} = -C_{\text{Mb}\alpha} - 2Sr(C_{L\alpha} + C_{Do}) \tag{A25f}$$

$$k_{43} = -\tfrac{1}{2} SL[(C_{D\alpha} - C_{Lo}) s_{\theta o} + (C_{L\alpha} + C_{Do}) c_{\theta o}] \tag{A25g}$$

$$k = \frac{2k^*}{\rho V_o^2 S^* L^*} \tag{A26a}$$

$$b = \frac{L^*}{V_o} \frac{2b^*}{\rho V_o S^* L^{*2}} \tag{A26b}$$

Note that the coefficients C_{Lo}, C_{Do}, $C_{L\alpha}$, and $C_{D\alpha}$ are the aerodynamic coefficients that correspond to the top-most boom in the two-boom configuration.

(Note that the form for M is for the fully linearized form.) As already mentioned, sometimes the quasi-linear form will need to be used. The quasi-linear form for the M matrix is

$$M = m_{\text{tot}} L^{*2} \begin{bmatrix} m_{11} & 0 & m_{23}q_3 & m_{14} + m_{24}q_3 + m_{24}q_4 & -m_{14} + m_{24}q_3 + m_{24}q_5 \\ 0 & m_{11} & m_{23} & m_{24} - m_{14}q_3 - m_{14}q_4 & m_{24} + m_{14}q_3 + m_{14}q_5 \\ m_{23}q_3 & m_{23} & m_{33} & m_{34} + m_{35}q_4 & m_{34} - m_{35}q_5 \\ m_{14} + m_{24}q_3 + m_{24}q_4 & m_{24} - m_{14}q_3 - m_{14}q_4 & m_{34} + m_{35}q_4 & m_{44} & 0 \\ -m_{14} + m_{24}q_3 + m_{24}q_5 & m_{24} + m_{14}q_3 + m_{14}q_5 & m_{34} - m_{35}q_5 & 0 & m_{44} \end{bmatrix} \tag{A27}$$

If one assumes that the mass ratio m is very, very small ($\ll 1$), then the inverse of M can be shown to be

$$M^{-1} = \frac{1}{m_{\text{tot}} L^{*2}} \begin{bmatrix} \frac{1}{m_{11}} & 0 & 0 & -\frac{m_{14}}{m_{11}m_{44}} & \frac{m_{14}}{m_{11}m_{44}} \\ 0 & \frac{1}{m_{11}} & -\frac{m_{23}m_{44} - 2m_{24}m_{34}}{m_{11}m_{33}m_{44}} & -\frac{m_{24}}{m_{11}m_{44}} & -\frac{m_{24}}{m_{11}m_{44}} \\ 0 & -\frac{m_{23}m_{44} - 2m_{24}m_{34}}{m_{11}m_{33}m_{44}} & \frac{1}{m_{33}} & -\frac{m_{34}}{m_{33}m_{44}} & -\frac{m_{34}}{m_{33}m_{44}} \\ -\frac{m_{14}}{m_{11}m_{44}} & -\frac{m_{24}}{m_{11}m_{44}} & -\frac{m_{34}}{m_{33}m_{44}} & \frac{1}{m_{44}} & \frac{m_{11}m_{34}^2 + m_{33}\left(m_{24}^2 - m_{14}^2\right)}{m_{11}m_{33}m_{44}^2} \\ \frac{m_{14}}{m_{11}m_{44}} & -\frac{m_{24}}{m_{11}m_{44}} & -\frac{m_{34}}{m_{33}m_{44}} & \frac{m_{11}m_{34}^2 + m_{33}\left(m_{24}^2 - m_{14}^2\right)}{m_{11}m_{33}m_{44}^2} & \frac{1}{m_{44}} \end{bmatrix} \tag{A28}$$

Equation (A18) can be written in linear form as

$$\begin{bmatrix} \dot{\boldsymbol{u}} \\ \dot{\boldsymbol{q}} \end{bmatrix} = \begin{bmatrix} M^{-1}B & M^{-1}K \\ G & 0 \end{bmatrix} \begin{bmatrix} \boldsymbol{u} \\ \boldsymbol{q} \end{bmatrix} + \begin{bmatrix} M^{-1}\boldsymbol{f}_o \\ 0 \end{bmatrix} \tag{A29}$$

where G is the differential relationship between the generalized coordinates and generalized velocities from Eqs. (A1a–A2e).

The results are in the state-space form of

$$\dot{\boldsymbol{x}} = A\boldsymbol{x} + \boldsymbol{x}_o \tag{A30}$$

which, when the operations in Eq. (A29) are carried out, will be in the form

$$\begin{bmatrix} \dot{u}_1 \\ \dot{u}_2 \\ \dot{u}_3 \\ \dot{u}_4 \\ \dot{u}_5 \\ \dot{q}_1 \\ \dot{q}_2 \\ \dot{q}_3 \\ \dot{q}_4 \\ \dot{q}_5 \end{bmatrix} = -\frac{1}{2}\frac{\rho V_o^2 S^*}{m_{\text{tot}} L^*} \left\{ \begin{bmatrix} a_{11} & a_{12} & 0 & a_{14} & -a_{14} & 0 & 0 & a_{18} & a_{19} & -a_{19} \\ 0 & a_{22} & a_{23} & a_{24} & a_{24} & 0 & 0 & a_{28} & a_{29} & a_{29} \\ 0 & a_{32} & a_{33} & a_{34} & a_{34} & 0 & 0 & a_{38} & a_{39} & a_{39} \\ a_{41} & a_{42} & a_{43} & a_{44} & a_{54} & 0 & 0 & a_{48} & a_{49} & a_{59} \\ -a_{41} & a_{52} & a_{43} & a_{54} & a_{44} & 0 & 0 & a_{58} & a_{59} & a_{49} \\ a_{61} & 0 & 0 & 0 & 0 & 0 & 0 & 0 & 0 & 0 \\ 0 & a_{61} & 0 & 0 & 0 & 0 & 0 & 0 & 0 & 0 \\ 0 & 0 & a_{83} & 0 & 0 & 0 & 0 & 0 & 0 & 0 \\ 0 & 0 & a_{83} & -a_{83} & 0 & 0 & 0 & 0 & 0 & 0 \\ 0 & 0 & a_{83} & 0 & -a_{83} & 0 & 0 & 0 & 0 & 0 \end{bmatrix} \begin{bmatrix} u_1 \\ u_2 \\ u_3 \\ u_4 \\ u_5 \\ q_1 \\ q_2 \\ q_3 \\ q_4 \\ q_5 \end{bmatrix} + \begin{bmatrix} x_{01} \\ 0 \\ 0 \\ x_{04} \\ -x_{04} \\ 0 \\ 0 \\ 0 \\ 0 \\ 0 \end{bmatrix} \right\} \tag{A31}$$

Acknowledgments

The authors thank the NASA Goddard Graduate Student Research Program, Technical Advisors Thomas Stengle and Michael Mesarch, and GEC Program Manager Paul Buchanan for their research opportunities and support.

References

[1]London, H. S., "Change of Satellite Orbit Plane by Aerodynamic Maneuvering," *Journal of the Aerospace Sciences*, Vol. 29, No. 2, 1962, pp. 323–332.

[2]Vinh, N. X., *Optimal Trajectories in Atmospheric Flight*, Elsevier, New York, 1981.

[3]Turner, J. D., and Chun, H. M., "Optimal Distributed Control of a Flexible Spacecraft During a Large-Angle Maneuver," *Journal of Guidance, Control, and Dynamics*, Vol. 7, No. 3, 1984, pp. 257–264.

[4]Budynas, R., and Poli, C., "Three-Dimensional Motion of a Large Flexible Satellite," *Automatica*, Vol. 8, Pergamon, Oxford, 1972, pp. 275–286.

[5]Moss, J. N., and Bird, G. A., "Direct Simulation of Transitional Flow for Hypersonic Reentry Conditions," AIAA Paper 84-0223, Jan. 1984.

[6]Lewis, M. J., "Aerodynamic Maneuvering for Stability and Control of Low-Perigee Satellites," *Advances in the Astronautical Sciences*, Vol. 108, Pt. 2, 2001, pp. 1927–1946.

[7]Bowman, D. S., "Numerical Optimization of Low-Perigee Spacecraft Shapes," M.S. Thesis, Aerospace Engineering Dept. UM-AERO 01-03, Univ. of Maryland, College Park, MD, 2001.

[8]Sentman, L. H., "Free Molecule Flow Theory and Its Application to the Determination of Aerodynamic Forces," Lockheed Missiles and Space Co., Tech. Rept. LMSC-448514, Sunnyvale, CA, Oct. 1961.

[9]Schultz, J. R., and Lewis, M. J., "Drag and Stability of a Low Perigee Satellite," American Astronautical Society, Paper 03-182, Feb. 2003.

[10]Kane, T. R., and Levinson, D. A., *Dynamics: Theory and Applications*, McGraw–Hill, New York, 1985.

[11]Ogata, K., *Modern Control Engineering*, 3rd ed., Prentice–Hall, Upper Saddle River, NJ, 1997, pp. 232–238.

[12]Anderson, J. D., *Introduction to Flight*, 3rd ed., McGraw–Hill, New York, 1989, pp. 375, 376.

[13]"Understanding Plasma Interactions with the Atmosphere: The Geospace Electrodynamic Connections (GEC) Mission," NASA TM-2001-209980, July 2001.

P. Weinacht
Associate Editor